Skilful forecasts of summer rainfall in the Yangtze River Basin from November

Philip E. BETT*[1], Nick DUNSTONE[1], Nicola GOLDING[1], Doug SMITH[1] and Chaofan LI[2,3]

[1] *Met Office Hadley Centre, FitzRoy Road, Exeter* EX1 3PB, *UK*

[2] *Center for Monsoon System Research, Institute of Atmospheric Physics, Chinese Academy of Sciences, Beijing 100029, China*

[3] *College of Earth and Planetary Sciences, University of the Chinese Academy of Sciences, Beijing 100049, China*

ABSTRACT

Variability in the East Asian Summer Monsoon (EASM) brings the risk of heavy flooding or drought to the Yangtze River Basin, with potentially devastating impacts. Early forecasts of the likelihood of enhanced or reduced monsoon rainfall can enable better management of water and hydropower resources by decision-makers, supporting livelihoods and major economic and population centres across Eastern China. This paper demonstrates that the EASM is predictable in a dynamical forecast model from the preceding November, and that this allows skilful forecasts of summer mean rainfall in the Yangtze River Basin at a lead time of 6 months. Skill for May–June–July rainfall is of a similar magnitude to seasonal forecasts initialised in spring, although the skill in June–July–August is much weaker and not consistently significant. However, there is some evidence for enhanced skill following El Niño events. The potential for decadal-scale variability in forecast skill is also examined, although we find no evidence for significant variation.

Key words: seasonal forecasting, interannual forecasting, flood forecasting, Yangtze basin rainfall, East Asian Summer Monsoon.

Article Highlights:

- The East Asian Summer Monsoon in MJJ can be skilfully predicted in a dynamical model initialised in November

- This can be used to forecast Yangtze River Basin summer rainfall using a simple linear regression model

- Skill in MJJ rainfall is comparable to seasonal forecasts at shorter lead times, but the skill in JJA is much lower.

- No evidence is found of decadal-scale variation in skill.

---

*Corresponding author: Philip BETT
Email: philip.bett@metoffice.gov.uk, twitter @pbett

1. Introduction

The Yangtze River basin is subject to heavy rainfall driven by the East Asian Summer Monsoon. This can lead to devastating floods, impacting the lives and livelihoods of millions of people, and leading to economic losses of ~100bn CNY (~10bn USD) and hundreds of deaths (e.g. Podlaha et al., 2016, 2020, 2021). The variability in seasonal and annual rainfall, and the need to take action to mitigate potential flooding, also has significant impact on the provision of hydroelectric power via some of the world's largest hydropower dams, feeding into the energy supply of eastern China's megacities.

In response to a user need for improved long-term prediction of this monsoonal variability (Golding, Hewitt, Zhang, et al., 2017), since 2016 the UK Met Office in collaboration with colleagues in China has developed a trial seasonal forecast system for Yangtze River basin summer rainfall (Bett et al., 2018), based on the GloSea seasonal forecast system (MacLachlan et al., 2015). Continued research, into user requirements for decision-making (Golding et al., 2019; Golding, Hewitt, & Zhang, 2017), climate predictability (e.g. Liu et al., 2018), as well as forecast evaluation and model changes, have led to improvements in the forecasts (Bett et al., 2020).

Currently, forecasts are produced each week from late winter until the summer, with forecasts for early summer (May–June–July, MJJ) being available from February and forecasts for high summer (June–July–August, JJA) available from March. Forecasts are delivered each month to the China Meteorological Administration (CMA), to be used as part of the overall forecast messages that are communicated to stakeholders, as well as being sent directly to specific users to elicit feedback. The forecasts are based on dynamical predictions of an East Asian Summer Monsoon index, supplemented by a linear regression to produce calibrated probabilistic forecasts of regional mean rainfall. The forecasts are skilful, and have performed well even under near-unprecedented extremes (Bett et al., 2021).

At the lead times currently available, hydropower dam operators are given sufficient warning of high flood seasons to be able to reduce water levels in the dams, and hence reduce the risk of flooding. Reducing the water levels over an extended period, before the rainfall occurs, limits the negative impacts on agriculture downstream, which is dependent on a steady availability of water, and maintains the continuous, stable provision of hydroelectric power to the electricity grid. However, a lead time of at most 3 months limits the value of the forecast to energy distributors, who plan the supply of electricity to cities and industry across Eastern China up to a year in advance, and are able to make use of longer lead times to protect the reliable provision of electricity. Hydroelectric dam operators are currently required to provide forecasts of electricity production on these longer timescales, and therefore a longer lead time forecast of rainfall for the main flood season would support this.

Improvements in interannual-to-decadal climate prediction (e.g. Cassou et al., 2018; Meehl et al., 2021; Merryfield et al., 2020; Smith et al., 2019) have opened the possibility of extending the lead time of seasonal climate services such as these beyond the periods available from traditional subseasonal-to-seasonal forecast systems (Dunstone et al., 2022). The Met Office Decadal Prediction System, DePreSys, has demonstrated high levels of skill in various features of the climate in the tropics and extratropics, at lead times beyond those of typical seasonal forecasts (Dunstone et al., 2016, 2018, 2020). DePreSys has also been shown to have some skill in forecasting East Asian Summer Monsoon rainfall in the extended summer, on short timescales (forecasts for JJAS initialised in May; Monerie et al., 2021) and longer timescales similar to our present investigation (forecasts for MJJAS initialised in November; Dunstone et al., 2020), as well as for the corresponding PMSL patterns over the West North Pacific. Other recent studies have also demonstrated the possibility of long-lead seasonal forecasts of summer rainfall in China, or the East Asian Summer Monsoon circulation more generally (Liu et al., 2021; Lu et al., 2012; Takaya et al., 2021).

Exploring how the skill of DePreSys in predicting the East Asian Summer Monsoon can be used to extend our Yangtze River basin rainfall forecasts to longer lead times, is a natural next step in the development of our climate service. In this paper, we shall therefore investigate the skill of forecasts of early summer and high summer rainfall over the Yangtze River basin, using the same method as the existing shorter-term seasonal forecasts, but based instead on dynamical forecasts initialised in November. This would double the current maximum lead time from 3 months to 6 months. In the following section we describe the data and methods we use for skill assessment, and we present our results in section 3. We summarise and discuss our results in section 4, and consider the prospects for improved climate services.

2. Data and methods

2.1 Hindcasts and observations

We use a set of hindcasts from the Met Office Decadal Climate Prediction System (DePreSys3, Dunstone et al., 2016, 2018). This is based on the Global Coupled 2 configuration of the HadGEM3 climate model (Williams et al., 2015), which is the same as used by the Met Office seasonal forecast system GloSea5. The DePreSys3 hindcasts consist of 40-member ensembles initialised each November from 1959 to 2018. We use the first summers in each of these forecasts, covering the 60-year period 1960–2019.

We use the 850 hPa zonal wind fields from the hindcasts to calculate the Wang & Fan (1999) EASM index, averaged over MJJ and JJA each year. This index characterises the anomalous circulation in the western North Pacific, as the mean zonal wind in a box in the South China Sea (5°–15° N, 90°–130° E) minus a box in the East China Sea (22.5°–32.5° N, 110°–140° E) (Bett et al., 2020; Wang et al., 2008). Low values correspond to anomalously anticyclonic circulation in the western North Pacific (an enhanced, i.e. westward-extended, West Pacific Subtropical High, WPSH), which acts to enhance the northward progress of the Meiyu monsoon front, resulting in more rainfall over the Yangtze basin. High values of the EASM index correspond to anomalously cyclonic circulation (a reduced WPSH), with moisture remaining over Southern China rather than progressing northwards over the Yangtze Basin. We have confirmed that our results are unchanged if we use a WPSH index; we retain the EASM index for consistency with previous work on Yangtze Basin seasonal forecast skill (Bett et al., 2020; Liu et al., 2018). We use the ERA5 reanalysis to calculate an observed EASM index over the same period, using the preliminary back-extension data for the pre-1979 period (Bell et al., 2020; Hersbach et al., 2019).

We use observed precipitation from the Global Precipitation Climatology Centre (GPCC) Full Data Monthly Product v2020 (Schneider et al., 2020). We calculate seasonal-mean regional-mean precipitation rates in three areas: the whole Yangtze River Basin itself, and two sub-basin regions defined by dividing the basin at 111° E: the Upper Reaches, and the Middle/Lower Reaches (following Bett et al., 2020). We label years as being El Niño, La Niña or neutral using the Niño3.4 SST anomalies in the December–January–February (DJF) preceding each summer, based on the Oceanic Nino Index (ONI)[2] data set, with a threshold of ±0.5 K.

2.2 Measures of skill, and regression-based forecasts

When assessing the skill of the DePreSys model output, a natural and simple first quantity to examine is the correlation of the ensemble-mean hindcasts with the observations, *r*. This measure of the standardized co-variability of the model with the observations is directly related to the linear regression approach we use for producing forecasts (see below): the hindcast–observation correlation provides a measure of skill for future forecasts (e.g. Bett et al., 2018, 2020). The uncertainty in the correlation is characterised by 95% confidence intervals calculated using a Fisher z-transformation; this corresponds to a two-sided test of statistical significance at the 5% level (both positive and negative correlations can be used to produce skilful forecasts, e.g. the EASM index is negatively correlated with Yangtze rainfall across most of the basin).

In this paper, we also wish to evaluate the skill of the linear regression-based probabilistic forecasts themselves, in addition to the above measure of model–observations correlation. The linear regression of the observed precipitation, against a predictor from the DePreSys ensemble-mean hindcast (in our case, the EASM index), characterises their mean historical relationship. When a new EASM forecast is produced from DePreSys, the prediction interval on the regression at that EASM value provides the rainfall forecast probability distribution. This method of producing probabilistic forecasts corrects for any bias in the mean and variance, and yields calibrated probabilities, by construction (Bett et al., 2022), within the sampling limits given by the number of years in the hindcast. This is an important limitation when using the operational GloSea hindcast, as that only covers 24 years (1993–2016). In contrast, the 60-year DePreSys hindcast allows statistically significant skill to be discernible from noise at a higher level of significance.

[2] https://origin.cpc.ncep.noaa.gov/products/analysis_monitoring/ensostuff/ONI_v5.php

To assess the skill of forecasts produced by this linear regression approach, we need to use leave-one-out cross-validation: we produce forecast probability density functions (PDFs) for each year in the hindcast period in turn, based on the regression relationship between the observations and hindcasts in the remaining 59 years. The correlation of the central estimates of these 60 cross-validated forecasts with the observations is a more stringent measure of forecast skill, reflecting the sensitivity to, and frequency of, outliers in the historical period. We will refer to this as the correlation skill, $\hat{r}$, and assess whether it is significantly greater than zero using a one-sided Fisher z-test (skilful regression-based forecasts can only be positively correlated with observations), again at the 5% level.

The performance of the forecast probability distributions themselves can be assessed using the continuous ranked probability score (CRPS, e.g. Hersbach, 2000; Wilks, 2020). For a given forecast, the CRPS is the integral of the squared differences between the forecast cumulative distribution function (CDF) and that of the observation that year (i.e. a step function CDF). The CRPS is therefore like a probabilistic forecast error: larger values indicate that more forecast probability is distributed further away from the observation. The CRPS from a proposed forecast model is compared with the CRPS from a reference forecast strategy: in our case, we use climatology, i.e. the CDF given by the distribution of 59 observations available when forecasting each year using cross-validation. The difference between the mean CRPS from the forecasts ($\overline{S_{\mathrm{fc}}}$) and that of the reference ($\overline{S_{\mathrm{ref}}}$), with respect to the difference between the perfect forecast score ($S_{\mathrm{perf}} = 0$) and the reference, is the corresponding skill score (CRPSS, e.g. Wilks, 2020):

$$\mathrm{CRPSS} = \frac{\overline{S_{\mathrm{fc}}} - \overline{S_{\mathrm{ref}}}}{S_{\mathrm{perf}} - \overline{S_{\mathrm{ref}}}} = 1 - \frac{\overline{S_{\mathrm{fc}}}}{\overline{S_{\mathrm{ref}}}}$$

Positive values indicate that the forecast is better than the reference strategy, and negative values mean that it is worse. We test for the forecast being significantly more skilful than climatology by using a one-sided paired t-test at the 5% level to compare the two mean CRPS values.

3. Results

3.1 Correlations between hindcasts and observations

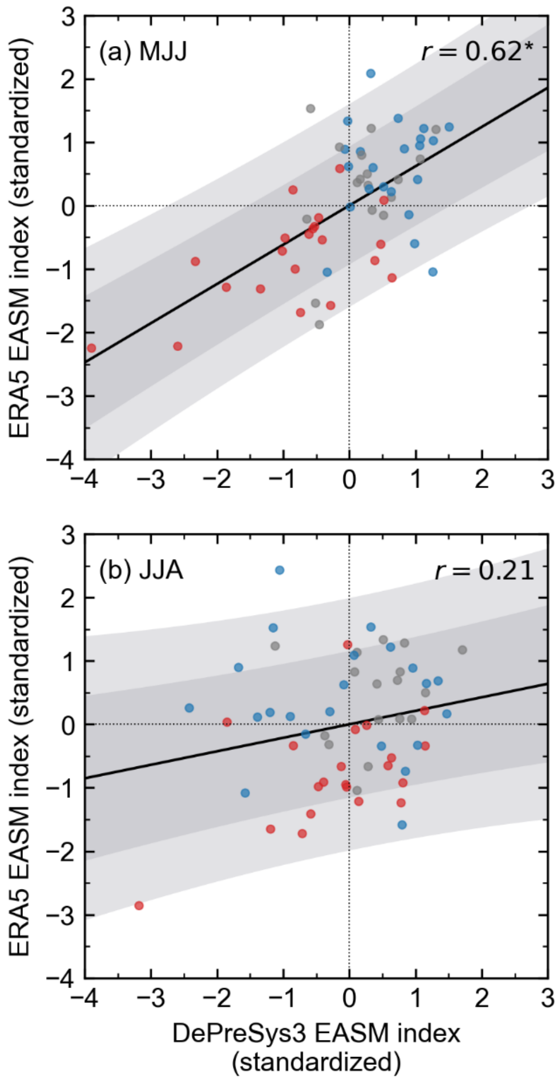

Figure 1. The relationship between the EASM index in observations, and in the DePreSys3 hindcasts initialised in November, for (a) MJJ and (b) JJA. Both panels include the correlations *r*, marked * where significant. Each point corresponds to a single summer, and is coloured according to ENSO, using the ONI during the preceding DJF: Red points correspond to El Niño and blue to La Niña. The diagonal black lines indicate the linear regression, and the surrounding grey shading shows the 75% and 95% prediction intervals based on that regression. The horizontal and vertical dotted lines indicate the mean values.

Figure 1 shows the correlation between the hindcast EASM index and the observed values from ERA5, reflecting the model skill in predicting the EASM. There is significant skill in early summer (MJJ, $r = 0.62$, with a p-value $< 2\times10^{-7}$), but not in JJA ($r = 0.21$, p-value 0.102). Both of these 6-month lead correlations are significantly weaker than those reported by Bett et al. (2020) for 1-month lead forecasts (0.87 for MJJ and 0.76 for JJA), as would be expected for longer lead times.

There is a clear indication of the influence of winter ENSO on the subsequent EASM: El Niño winters tend to result in negative EASM indices in MJJ, and La Niña winters tend to result in positive EASM indices. However, this relationship is much stronger for the El Niño side: if we select the 21 El Niño years only, the correlation barely changes ($r = 0.59$, $p = 0.004$), while for the 22 La Niña years $r = 0.08$. ENSO-neutral years yield $r = 0.41$, with $p = 0.105$. Selecting all ENSO-active years (following El Niños or La Niñas) yields a correlation of $r = 0.66$ ($p < 7\times10^{-7}$), which is also very similar to selecting all years. Furthermore, although there is no significant skill overall for JJA, the skill in El Niño years is much better: $r = 0.50$, significant with $p = 0.02$. The JJA monsoon index correlations following La Niña, ENSO-neutral or ENSO-active winters remain not statistically significant (r = -0.1, 0.18 and 0.14 respectively).

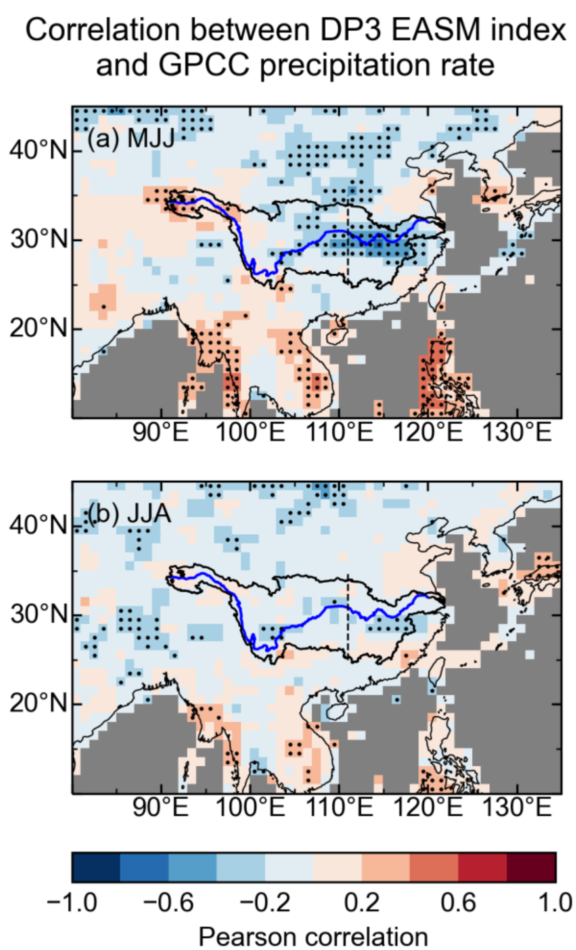

Figure 2. Correlation between observed rainfall and hindcast EASM index in MJJ and JJA. The Yangtze River is shown as a blue line, with its basin outlined in black, and the division between the Upper and Middle/Lower Reaches is shown with a vertical dashed black line. Stippling marks areas where the correlation is significantly different to zero.

In Figure 2 we map the correlation between the forecast EASM index and the observed precipitation. As expected from Figure 1, we can identify some areas of significant correlation in the Yangtze River basin in MJJ, mostly but not exclusively in the Middle and Lower Reaches. In contrast, the correlations are much weaker in JJA.

Building on these results, we show scatter plots describing the relationship between the DePreSys EASM index and regional-mean MJJ precipitation in Figure 3. Although the correlations in all three regions are statistically significant, that for the Upper Reaches remains rather small ($|r| < 0.4$) and may be of marginal use for decision-makers, depending on their particular requirements.

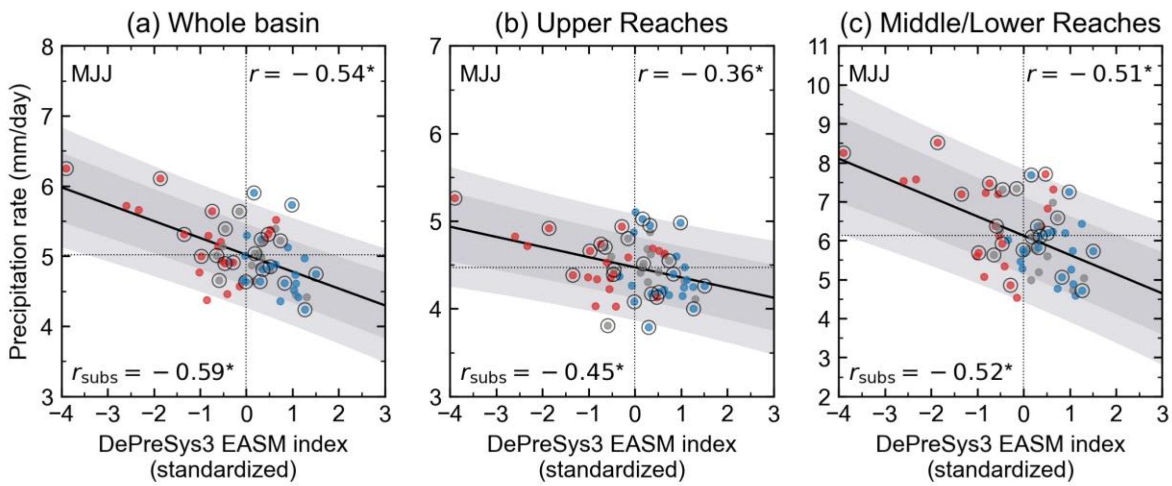

Figure 3. Relationships between observed regional-mean MJJ rainfall and the hindcast EASM index. Correlations using all 60 years are marked in the top-right of each panel (r), and correlations based on the 24-year subset 1993–2016 are shown in the bottom-left (r_{subs}; points in that subset are circled). As in Figure 1, points are colour-coded according to ENSO in the preceding winter, red for El Niño, blue for La Niña. The linear regression is shown by the black line, surrounded by shading giving the 75% and 95% prediction intervals. Horizontal and vertical dotted lines give the mean values over all 60 years.

As with Figure 1, Figure 3 shows a clear relationship with ENSO. For the MJJ results shown, picking out the 21 El Niño years only yields significant correlations for the whole basin ($r = -0.53$, $p = 0.011$) and the Upper Reaches ($r = -0.50$, $p = 0.021$), while the correlation is reduced for the Middle/Lower Reaches ($r = -0.42$, $p = 0.054$). In contrast, none of the regions show significant correlations for the subset of 22 La Niña years ($p > 0.15$ in all cases). These results highlight the importance of conditional skill in these cases – e.g. although the correlation in MJJ for the Upper Reaches might be too low to be useful in most years, the forecasts could be much more valuable following an El Niño.

This is also true for the JJA results (not shown). For the whole basin, the correlation is -0.29 ($p = 0.026$), i.e. just significant at the 5% level. For the sub-basin regions the correlations are weaker still, with $|r| < 0.25$. However, in the case of the Upper Reaches, in the summers following El Niño events the correlation strengthens to -0.49 (p = 0.022), similar to the values for MJJ.

We have also tested the impact of the longer hindcast period available from DePreSys (60 years) compared to GloSea (24 years). In Figure 3, the subset of years comprising the GloSea hindcast period (1993–2016) are highlighted, and the correlations based on those subsets alone are labelled as r_{subs}. Although the 24-year correlations all appear slightly stronger, these differences are not statistically significant, and the longer period gives the more robust estimates of skill: for example, the confidence intervals on the 24-year correlations are much wider, or equivalently, 60 years allows weaker correlations to be more robustly determined as statistically significant (for a given significance level). Again considering the whole-basin correlation for JJA (not shown), the 60-year correlation of -0.29 has a 95% confidence interval of -0.50 to -0.03, i.e. significant at the 5% level as described above. Using 24 years, the central estimate is relatively unchanged (-0.33), but its confidence interval is now -0.64 to +0.09, i.e. statistically indistinguishable from zero at the 5% level.

It seems clear from our results that the greatest prospects for significant and usable forecast skill using our method will be from MJJ for the Middle and Lower Reaches, and for the basin as a whole, although following an El Niño event forecasts for rainfall in the Upper Reaches of the basin should also be considered.

3.2 Cross-validated skill from linear regression

Figure 4 shows the rainfall forecasts produced by linear regression with leave-one-out cross-validation, for the whole basin in MJJ. The correlation skill of the forecast central estimate ($\hat{r}$), and the probabilistic skill (CRPSS) are both statistically significant at the 5% level (p = 0.00002 and 0.03 respectively), showing that the forecasts represent an improvement over simply using the climatological distribution. It is important to note that the forecast uncertainty (in terms of the prediction intervals) remains of a similar size to the observed interannual variability, and there are two occasions where the observation lies outside the 95% prediction interval (as expected from 60 forecasts).

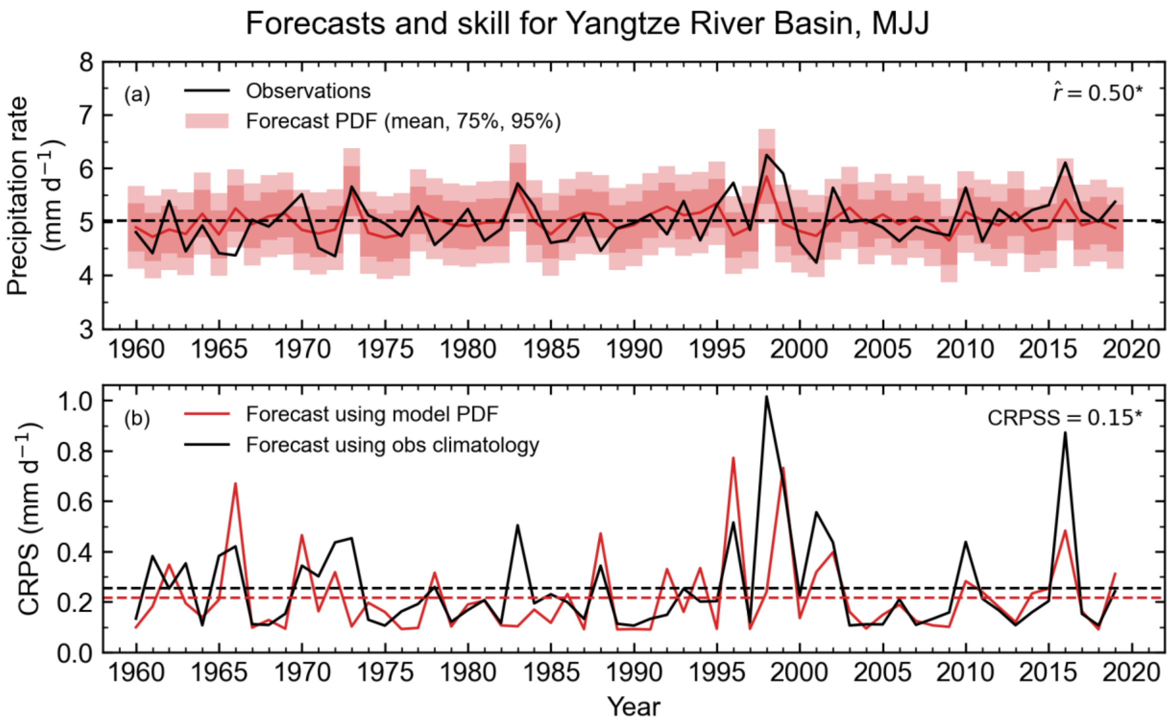

Figure 4. Time series showing forecast skill, using forecasts of MJJ rainfall in the Yangtze River basin. Top (a): timeseries of the forecast PDFs (pink, in terms of the forecast mean, and 75% and 95% prediction intervals) and observations (black), showing the correlation skill $\hat{r}$, marked with a * indicating it is significantly greater than zero. Bottom (b): timeseries of CRPS values based on using the model PDF for the forecast (red), or using the observed climatology as the forecast (black). The corresponding skill score is shown (CRPSS), comparing the mean CRPS from the two forecast strategies (red and black dashed lines); the * indicates the model-based forecast is significantly better than using climatology.

The climatology-based CRPS time series naturally shows notable spikes (increased error) in the more extreme years, as by definition those years are not present in the distribution used for the "forecast". The DePreSys-based forecasts perform much better in most of these cases (having smaller CRPS values), demonstrating the ability of the dynamical model to produce out-of-sample forecasts.

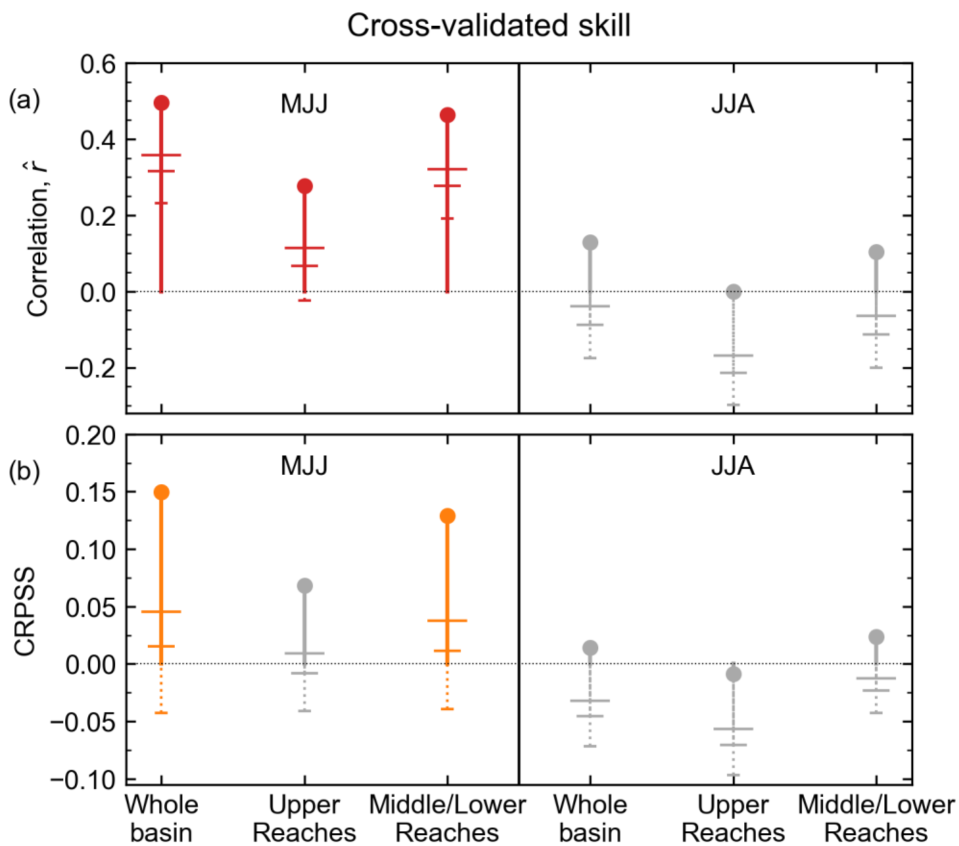

Figure 5. Summary of regional skill for MJJ and JJA. Coloured points indicate the skill is significantly greater than zero at the 5% level, i.e. the forecasts are significantly better than using climatology; grey points indicate the skill is statistically indistinguishable from zero at that level. Long, medium and short horizontal ticks on each line indicate the lower limits of the one-sided confidence intervals at the 90%, 95% and 99% levels respectively.

Figure 5 summarises the correlation skill and CRPSS for rainfall in MJJ and JJA across all three regions. Consistent with our previous results, there is no significant skill in JJA. The correlation skill for the Upper Reaches in MJJ is statistically significant ($p = 0.016$) but low (0.28), and the corresponding CRPSS of 0.068 indicates the forecasts are not significantly better than using climatology ($p = 0.07$).

The cross-validation of these skill scores makes them more sensitive to the number of contributing years. When we subset according to whether the summer follows an El Niño or La Niña (as in the previous subsection), we find that only the correlation skill in MJJ for the whole basin remains significant ($\hat{r} = 0.38$, $p = 0.046$). All other correlation skill is worse under El Niño conditions ($p > 0.1$ for MJJ, $p > 0.5$ for the JJA cases), and La Niña conditions ($p > 0.3$ in all cases). None of the CRPSS values are significant when subselecting by El Niño ($p > 0.1$) or La Niña conditions ($p > 0.4$).

3.3 Potential variation in skill

The length of the hindcast period available from DePreSys raises the question of whether decadal-scale climate variability could affect the forecast skill, and if there would be a benefit in focusing on the most recent 20–30-year period as typically used by seasonal forecasting systems. In our case, as in section 3.1, we will be comparing with the 24-year period used by GloSea, for consistency with our earlier results.

Figure 6 shows the correlations between EASM index and Yangtze basin rainfall in MJJ for observations, and for the EASM hindcasts, using rolling 24-year windows within the 60-year hindcast period. The observed correlation appears to weaken slightly over time: it is approximately -0.8 for the earliest window (1960–1983), but approximately -0.5 for the latest period (1995–2019), for example. However, the confidence intervals (uncertainty ranges) on correlations based on 24 years are relatively large, and these values are not significantly different to each other (p = 0.086). It is not surprising therefore that the correlation between model hindcast and observations does not show similar changes.

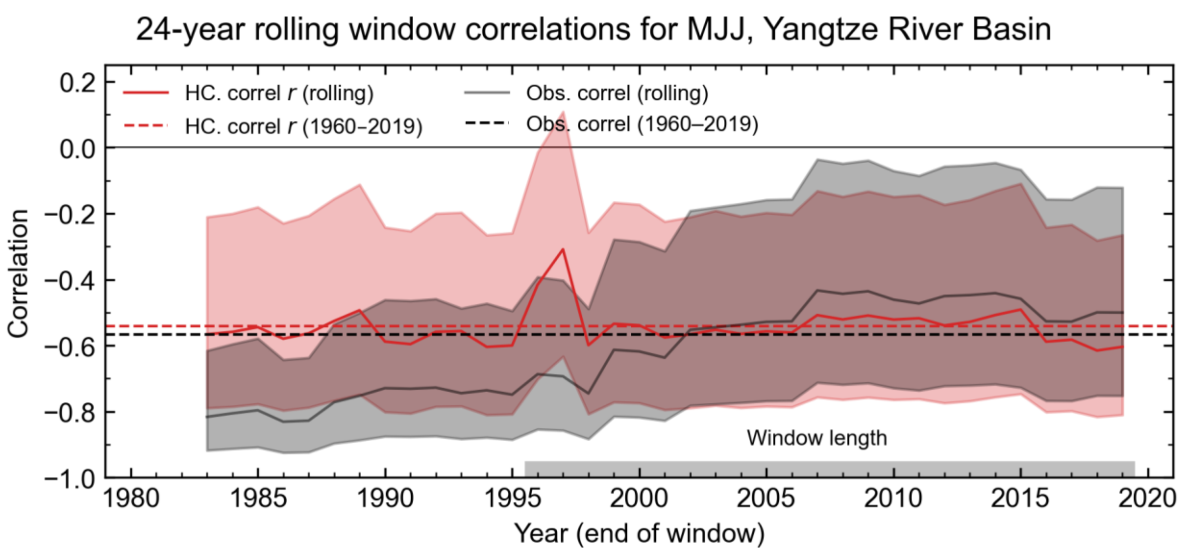

Figure 6. The variability in the relationship between EASM and Yangtze River basin rainfall in MJJ, in terms of correlations in 24-year rolling windows. The black line shows the observed EASM–rainfall correlation, with grey shading indicating the 95% confidence intervals. The red line and shading shows the same, but for hindcasts of the EASM correlated with the observed rainfall (cf. Figure 3). The window length is indicated by a grey box, as labelled. Points are plotted at the final year of each window. The correlations based on the full 60-year hindcast period are marked as dashed horizontal lines.

The results for the Middle and Lower Reaches in MJJ (not shown) are similar to those seen in Figure 6, but with some periods where the observed correlation was not significant at the 5% level. The results for the Upper Reaches in MJJ, and for all regions in JJA, show much more variability and fewer periods of significance, particularly for the hindcast–observations correlations, as expected from there being little/no significant skill overall.

These results do not show convincing evidence of variation in skill, which gives us confidence in our use of the full 60-year hindcast period in our forecasts. It also further illustrates the benefit of longer hindcast periods when assessing and calibrating seasonal-to-interannual forecasts.

4. Discussion and Conclusions

We have shown that DePreSys3 can skilfully forecast the EASM index in MJJ from November, and that this leads to skilful forecasts of rainfall in MJJ in the Middle and Lower Reaches of the Yangtze River basin, and for the basin as a whole. In contrast to similar seasonal forecasts initialised in the spring, we find no significant levels of skill in forecasting the EASM index, or Yangtze rainfall, in JJA. However, we do find some indications of enhanced skill in the Upper Reaches of the basin in both MJJ and JJA following El Niño events.

The EASM index we use captures the influence of sea surface temperatures (SSTs) in both the Pacific and the Indian Oceans on monsoon circulation and rainfall (Li et al., 2021; Liu et al., 2018; Takaya et al., 2021; Wang et al., 2008). As the Indian Ocean is able to store the impact of El Niño events, helping to persist their influence over an additional year (the Indian Ocean "capacitor" effect, e.g. Takaya et al., 2021; Xie et al., 2016), it is perhaps no surprise that the East Asian Summer Monsoon retains predictability at very long lead times. Indeed, Takaya et al. (2021) demonstrated forecast skill in the EASM index in JJA from April in the preceding year, using a dynamical model similar to ours.

A possibility for further extending our seasonal forecasts is to expand the statistical model component to use multiple predictors, which might retain predictability at longer lead times, or capture additional variability at lead times already explored. Obvious choices are SST indices, like a combination of Nino3.4, and the Indian Ocean Dipole (IOD) or Basin-wide indices (IOB). For example, Dunstone et al. (2020) has already shown that DePreSys retains skill in forecasting ENSO into the second winter after initialisation. Liu et al. (2021) take a very similar approach to us, using November initialisations to forecast JJA rainfall over southern China (overlapping the Yangtze basin), but use two predictor indices: SSTs in the Western North Pacific, and PMSL over a large area stretching from the tropical WNP down to Australia. This suggests that our poor skill for JJA might be improved by including better predictors. Pan & Lu (2022) have made a detailed study of predictors based on Pacific and Indian Ocean temperature and atmospheric circulation, which may help with predictability of the WPSH in July.

Another possibility, albeit more speculative, is to introduce extratropical predictors. The extreme rainy season of 2020 highlighted the capacity of midlatitude climate features such as the East Asian Jet to enhance the effect of the monsoon circulation captured by the EASM index (e.g. Bett et al., 2021; Li et al., 2021; and references therein). The summer NAO, for example, has a well-known teleconnection to the East Asian summer monsoon (e.g. Linderholm et al., 2011), but it is also known that extratropical dynamical climate features such as this remain largely unpredictable in current forecasting systems (Dunstone et al., 2018). However, Han & Zhang (2022) have shown that the *winter* NAO has an impact on April/May rainfall in the Middle/Lower Reaches of the Yangtze basin, so including the NAO from the first or even second winter (Dunstone et al., 2016) may improve the forecasts for MJJ.

Our results show a clear benefit from having a long, 60-year hindcast period, as the assessed skill when using a shorter period can be notably affected by the inclusion/exclusion of particular extreme years. The longer hindcast also allows a more robust assessment of probabilistic skill scores like the CRPSS, which require more data to demonstrate a significant level of skill. However, when using such long periods, it is important to consider whether the skill varies over that period, particularly in the context of a changing climate. For example, many studies have shown decadal-scale variability in ENSO, and its predictability (e.g. Hou et al., 2022; Tang et al., 2008; Weisheimer et al., 2022; and references therein), and similarly for the EASM and WPSH (e.g. Li et al., 2016; Y. Zhang et al., 2022; Z. Zhang et al., 2018). Several studies have shown that summer rainfall in Eastern China is itself subject to decadal-scale variability (e.g. Yang et al., 2017; Zhang et al., 2018; Zhu et al., 2016). However, we have shown that, for the specific case of EASM-based Yangtze summer rainfall, there is no significant variability in skill.

Decision-makers in the hydroelectric dams along the Yangtze River and its tributaries are able to use long-range seasonal forecasts to prepare flood mitigation actions and estimate their energy production, allowing water and electricity resources to remain relatively stable and be well-managed in the event of an extreme flood or drought season. Forecasts of Yangtze River basin rainfall from November developed here could allow action to be taken with greater confidence, on timescales that match existing planning decisions.

Acknowledgments. This work and its contributors were supported by the UK-China Research & Innovation Partnership Fund through the Met Office Climate Science for Service Partnership (CSSP) China as part of the Newton Fund. This paper contains modified Copernicus Climate Change Service information (2021), and neither the European Commission nor ECMWF is responsible for any use that may be made of that Copernicus information or data.

REFERENCES

Bell, B., Hersbach, H., Berrisford, P., Dahlgren, P., Horányi, A., Muñoz Sabater, J., et al. (2020). ERA5 monthly averaged data on pressure levels from 1950 to 1978 (preliminary version). Copernicus Climate Change Service (C3S) Climate Data Store (CDS). Retrieved from https://cds.climate.copernicus-climate.eu/cdsapp#!/dataset/reanalysis-era5-pressure-levels-monthly-means-preliminary-back-extension?tab=overview

Bett, P. E., Scaife, A. A., Li, C., Hewitt, C., Golding, N., Zhang, P., et al. (2018).

Seasonal Forecasts of the Summer 2016 Yangtze River Basin Rainfall. *Advances in Atmospheric Sciences*, *35*(8), 918–926. https://doi.org/10.1007/s00376-018-7210-y

Bett, P. E., Martin, N., Scaife, A. A., Dunstone, N., Martin, G. M., Golding, N., et al. (2020). Seasonal Rainfall Forecasts for the Yangtze River Basin of China in Summer 2019 from an Improved Climate Service. *Journal of Meteorological Research*, *34*(5), 904–916. https://doi.org/10.1007/s13351-020-0049-z

Bett, P. E., Martin, G. M., Dunstone, N., Scaife, A. A., Thornton, H. E., & Li, C. (2021). Seasonal Rainfall Forecasts for the Yangtze River Basin in the Extreme Summer of 2020. *Advances in Atmospheric Sciences*, *38*(12), 2212–2220. https://doi.org/10.1007/s00376-021-1087-x

Bett, P. E., Thornton, H. E., Troccoli, A., Felice, M. De, Suckling, E., Dubus, L., et al. (2022). *A simplified seasonal forecasting strategy, applied to wind and solar power in Europe*. *Climate Services* (Vol. 27). Elsevier. https://doi.org/10.1016/J.CLISER.2022.100318

Cassou, C., Kushnir, Y., Hawkins, E., Pirani, A., Kucharski, F., Kang, I. S., & Caltabiano, N. (2018). Decadal climate variability and predictability: Challenges and opportunities. *Bulletin of the American Meteorological Society*, *99*(3), 479–490. https://doi.org/10.1175/BAMS-D-16-0286.1

Dunstone, N., Smith, D., Scaife, A., Hermanson, L., Eade, R., Robinson, N., et al. (2016). Skilful predictions of the winter North Atlantic Oscillation one year ahead. *Nature Geoscience*, *9*(11), 809–814. https://doi.org/10.1038/ngeo2824

Dunstone, N., Smith, D., Scaife, A., Hermanson, L., Fereday, D., O'Reilly, C., et al. (2018). Skilful Seasonal Predictions of Summer European Rainfall. *Geophysical Research Letters*. https://doi.org/10.1002/2017gl076337

Dunstone, N., Smith, D., Yeager, S., Danabasoglu, G., Monerie, P. A., Hermanson, L., et al. (2020). Skilful interannual climate prediction from two large initialised model ensembles. *Environmental Research Letters*, *15*(9), 094083. https://doi.org/10.1088/1748-9326/ab9f7d

Dunstone, N., Lockwood, J., Solaraju-Murali, B., Reinhardt, K., Tsartsali, E. E., Athanasiadis, P. J., et al. (2022). Towards useful decadal climate services. *Bulletin of the American Meteorological Society*, *103*(7), E1705–E1719. https://doi.org/10.1175/BAMS-D-21-0190.1

Golding, N., Hewitt, C., & Zhang, P. (2017). Effective engagement for climate services: Methods in practice in China. *Climate Services*, *8*, 72–76. https://doi.org/10.1016/j.cliser.2017.11.002

Golding, N., Hewitt, C., Zhang, P., Bett, P., Fang, X., Hu, H., & Nobert, S. (2017). Improving user engagement and uptake of climate services in China. *Climate Services*, *5*, 39–45. https://doi.org/10.1016/j.cliser.2017.03.004

Golding, N., Hewitt, C., Zhang, P., Liu, M., Zhang, J., & Bett, P. (2019). Co-development of a seasonal rainfall forecast service: Supporting flood risk management for the Yangtze River basin. *Climate Risk Management*. https://doi.org/https://doi.org/10.1016/j.crm.2019.01.002

Han, J., & Zhang, R. (2022). Influence of preceding North Atlantic Oscillation on the spring precipitation in the middle and lower reaches of the Yangtze River valley. *International Journal of Climatology*, *42*(9), 4728–4739. https://doi.org/10.1002/joc.7500

Hersbach, H. (2000). Decomposition of the continuous ranked probability score for ensemble prediction systems. *Weather and Forecasting*, *15*(5), 559–570. https://doi.org/10.1175/1520-0434(2000)015<0559:DOTCRP>2.0.CO;2

Hersbach, H., Bell, B., Berrisford, P., Biavati, G., Horányi, A., Muñoz Sabater, J., et al. (2019). ERA5 monthly averaged data on pressure levels from 1979 to present. Copernicus Climate Change Service (C3S) Climate Data Store (CDS). https://doi.org/10.24381/cds.6860a573

Hou, Z., Li, J., Ding, R., & Feng, J. (2022). Investigating decadal variations of the seasonal predictability limit of sea surface temperature in the tropical Pacific. *Climate Dynamics*, *59*(3–4), 1079–1096. https://doi.org/10.1007/s00382-022-06179-3

Li, C., Lu, R., & Dong, B. (2016). Interdecadal changes on the seasonal prediction of the western North Pacific summer climate around the late 1970s and early 1990s. *Climate Dynamics*, *46*(7–8), 2435–2448. https://doi.org/10.1007/s00382-015-2711-1

Li, C., Lu, R., Dunstone, N., Scaife, A. A., Bett, P. E., & Zheng, F. (2021). The Seasonal Prediction of the Exceptional Yangtze River Rainfall in Summer 2020. *Advances in Atmospheric Sciences*. https://doi.org/10.1007/s00376-021-1092-0

Linderholm, H. W., Ou, T., Jeong, J. H., Folland, C. K., Gong, D., Liu, H., et al. (2011). Interannual teleconnections between the summer North Atlantic Oscillation and the East Asian summer monsoon. *Journal of Geophysical Research Atmospheres*, *116*(13), D13107. https://doi.org/10.1029/2010JD015235

Liu, Y., Ren, H., Scaife, A. A., & Li, C. (2018). Evaluation and Statistical Downscaling of East Asian Summer Monsoon Forecasting in BCC and MOHC Seasonal Prediction Systems. *Quarterly Journal of the Royal Meteorological Society*, *144*(717), 2798–2811. https://doi.org/10.1002/qj.3405

Liu, Y., Ren, H. L., Klingaman, N. P., Liu, J., & Zhang, P. (2021). Improving long-lead seasonal forecasts of precipitation over Southern China based on statistical downscaling using BCC_CSM1.1m. *Dynamics of Atmospheres and Oceans*, *94*, 101222. https://doi.org/10.1016/j.dynatmoce.2021.101222

Lu, R.-Y., Li, C.-F., Yang, S. H., & Dong, B. (2012). The Coupled Model Predictability of the Western North Pacific Summer Monsoon with Different Leading Times. *Atmospheric and Oceanic Science Letters*, *5*(3), 219–224. https://doi.org/10.1080/16742834.2012.11447000

MacLachlan, C., Arribas, A., Peterson, K. A., Maidens, A., Fereday, D., Scaife, A. A., et al. (2015). Global Seasonal forecast system version 5 (GloSea5): a high-resolution seasonal forecast system. *Quarterly Journal of the Royal Meteorological Society*, *141*(689), 1072–1084. https://doi.org/10.1002/qj.2396

Meehl, G. A., Richter, J. H., Teng, H., Capotondi, A., Cobb, K., Doblas-Reyes, F., et al.

(2021, May 1). Initialized Earth System prediction from subseasonal to decadal timescales. *Nature Reviews Earth and Environment*. Springer Nature. https://doi.org/10.1038/s43017-021-00155-x

Merryfield, W. J., Baehr, J., Batté, L., Becker, E. J., Butler, A. H., Coelho, C. A. S., et al. (2020). Current and Emerging Developments in Subseasonal to Decadal Prediction. *Bulletin of the American Meteorological Society*, *101*(6), E869--E896. https://doi.org/10.1175/bams-d-19-0037.1

Monerie, P. A., Robson, J. I., Dunstone, N. J., & Turner, A. G. (2021). Skilful seasonal predictions of global monsoon summer precipitation with DePreSys3. *Environmental Research Letters*, *16*(10), 104035. https://doi.org/10.1088/1748-9326/ac2a65

Pan, M., & Lu, M. (2022). Long-Lead Predictability of Western North Pacific Subtropical High. *Journal of Geophysical Research: Atmospheres*, *127*(5), e2021JD035967. https://doi.org/10.1029/2021JD035967

Podlaha, A., Bowen, S., & Darbinyan, C. (2016). *Global Catastrophe Recap: July 2016*. Retrieved from https://www.aon.com/reinsurance/thoughtleadership/default.jsp

Podlaha, A., Bowen, S., Lörinc, M., Kerschner, B., & Srivastava, G. (2020). *Global Catastrophe Recap: September 2020*. Retrieved from https://www.aon.com/reinsurance/thoughtleadership/default.jsp

Podlaha, A., Bowen, S., Lörinc, M., & Kerschner, B. (2021). *Global Catastrophe Recap: September 2021*. Retrieved from https://www.aon.com/reinsurance/thoughtleadership/default.jsp

Schneider, U., Becker, A., Finger, P., Rustemeier, E., & Ziese, M. (2020). GPCC Full Data Monthly Product Version 2020 at 1.0°: Monthly Land-Surface Precipitation from Rain-Gauges built on GTS-based and Historical Data. Deutscher Wetterdienst. https://doi.org/10.5676/DWD_GPCC/FD_M_V2020_100

Smith, D. M., Eade, R., Scaife, A. A., Caron, L. P., Danabasoglu, G., DelSole, T. M., et al. (2019). Robust skill of decadal climate predictions. *Npj Climate and Atmospheric Science*, *2*(1), 1–10. https://doi.org/10.1038/s41612-019-0071-y

Takaya, Y., Kosaka, Y., Watanabe, M., & Maeda, S. (2021). Skilful predictions of the Asian summer monsoon one year ahead. *Nature Communications*, *12*(1). https://doi.org/10.1038/s41467-021-22299-6

Tang, Y., Deng, Z., Zhou, X., Cheng, Y., & Chen, D. (2008). Interdecadal variation of ENSO predictability in multiple models. *Journal of Climate*, *21*(18), 4811–4833. https://doi.org/10.1175/2008JCLI2193.1

Wang, B., & Fan, Z. (1999). Choice of South Asian Summer Monsoon Indices. *Bulletin of the American Meteorological Society*, *80*(4), 629–638. https://doi.org/10.1175/1520-0477(1999)080<0629:COSASM>2.0.CO;2

Wang, B., Wu, Z., Li, J., Liu, J., Chang, C.-P., Ding, Y., & Wu, G. (2008). How to Measure the Strength of the East Asian Summer Monsoon. *Journal of Climate*, *21*(17), 4449–4463. https://doi.org/10.1175/2008jcli2183.1

Weisheimer, A., Balmaseda, M. A., Stockdale, T. N., Mayer, M., Sharmila, S., Hendon, H., & Alves, O. (2022). Variability of ENSO Forecast Skill in 2-Year Global Reforecasts Over the 20th Century. *Geophysical Research Letters*, *49*(10), e2022GL097885. https://doi.org/10.1029/2022gl097885

Wilks, D. S. (2020). Forecast Verification. In *Statistical Methods in the Atmospheric Sciences* (Fourth edi, pp. 369–483). Elsevier. https://doi.org/10.1016/b978-0-12-815823-4.00009-2

Williams, K. D., Harris, C. M., Bodas-Salcedo, A., Camp, J., Comer, R. E., Copsey, D., et al. (2015). The Met Office Global Coupled model 2.0 (GC2) configuration. *Geoscientific Model Development*, *8*(5), 1509–1524. https://doi.org/10.5194/gmd-8-1509-2015

Xie, S.-P. P., Kosaka, Y., Du, Y., Hu, K., Chowdary, J. S., & Huang, G. (2016). Indo-western Pacific ocean capacitor and coherent climate anomalies in post-ENSO summer: A review. *Advances in Atmospheric Sciences*, *33*(4), 411–432. https://doi.org/10.1007/s00376-015-5192-6

Yang, Q., Ma, Z., Fan, X., Yang, Z. L., Xu, Z., & Wu, P. (2017). Decadal modulation of precipitation patterns over eastern China by sea surface temperature anomalies. *Journal of Climate*, *30*(17), 7017–7033. https://doi.org/10.1175/JCLI-D-16-0793.1

Zhang, Y., Wang, W., Ding, R., Li, J., & Sun, C. (2022). Modulation of the predictability of the East Asian summer monsoon by the interdecadal Pacific oscillation. *Journal of Geophysical Research: Atmospheres*, e2021JD035903. https://doi.org/10.1029/2021JD035903

Zhang, Z., Sun, X., & Yang, X. Q. (2018). Understanding the interdecadal variability of East Asian summer monsoon precipitation: Joint influence of three oceanic signals. *Journal of Climate*, *31*(14), 5485–5506. https://doi.org/10.1175/JCLI-D-17-0657.1

Zhu, Y., Wang, T., & Ma, J. (2016). Influence of internal decadal variability on the summer rainfall in Eastern China as simulated by CCSM4. *Advances in Atmospheric Sciences*, *33*(6), 706–714. https://doi.org/10.1007/s00376-016-5269-x